Geomechanics from Micro to Macro – Soga et al. (Eds)
© 2015 Taylor & Francis Group, London, ISBN 978-1-138-02707-7

Incorporation of initial static shear stress in the dilatancy flow rule of granular materials under quasi-static loading

Homayoun Shaverdi
Civil Engineering Department, Ilam University, Iran

Frazin Kalantary
Department of Geotechnical Engineering, Khaje Nasir Toosi University of Technology, Iran

Mohd Raihan Taha
Civil and Structural Engineering Department, Universiti Kebangsaan Malaysia (UKM), Malaysia

ABSTRACT: Behavior of granular materials under static and cyclic loading is affected by inherent as well as induced anisotropy. In this paper, the effect of induced anisotropy due to initial static shear stress on quasi-static loading is studied. New dilatancy formulation is developed in a micro-level analysis, which also includes non-coaxiality and fabric anisotropy. The stress, strain and fabric non-coaxialities are attributed to stress-fabric and strain-fabric. The validity of the proposed formulation is examined by simulation of experimental data.

1 INTRODUCTION

The different behaviors of granular soils previously have been attributed to the density and confining pressure. However, recent studies showed that more than density and confining pressure have to be considered to interpret the behavior of granular soils. Experimental data showed that initial fabric anisotropy (or bedding angle) has a dominant effect on the behavior of soils (e.g., Vaid & Chern, 1983, Arangelovski & Towata, 2004). The initial static shear stress cause the rotation of principal stresses and it in turn cause the non-coaxiality between stress and the deposition angle (Oda, 1972, Yoshimine et al., 1998). This rotation and non-coaxiality between stress and fabric result in non-coaxiality between stress and strain. The initial static shear stress is tantamount to the non-coaxiality between the stress and fabric tensors.

Some facilities such as dams, slopes and foundation of buildings develop large distortion and settlements when they are subjected to seismic forces. Back-analysis of the failure of Sanfernando dam revealed that only 35 percent of the laboratory triaxial compression value was developed along the failure surface (Finn 2000). Deformations and damages on quay walls during the Kobe earthquake showed that significant lateral movement occurred in the area with or without liquefaction. These observations (damages and deformations) cannot be fitted into the established theory of critical state soil mechanics in which the critical state shear strength of a soil is a function only of its density (Li & Dafalias 2004). The difference between reality and experimental is due to the effect of initial static shear stress in the reality case and luck of this in the laboratory tests (Finn et al., 1982, Vaid & Sivathalayan, 1996). Several studies showed that initial void ratio, confining pressure and initial static shear stress (or bedding angle) are the major initial state variables (Vaid et al., 2001). For this reason these two effects (Fabric and non-coaxiality) must be included into dilatancy formulation of soils.

2 THEORETICAL FORMULATION

In the micro-level analysis by using the energy principles for granular soils Shaverdi et al. (2014) showed that:

$$\sigma_{ij}\,\dot{\varepsilon}_{ij} = \oint E(\theta) f_i d_j \, d\Omega = \dot{\tilde{\psi}} \tag{1}$$

where $\dot{\tilde{\psi}}$ is the dissipation function and σ_{ij} is the Cauchy stress, ε_{ij} its strain counterpart, f_i is the internal force, d_j is relative displacements of contact points and $E(\theta)$ is the distribution function of the contacts. Using micro-level parameters and some algebra the following equation was proposed for dilatancy:

$$\bar{d} = \frac{1}{1 - F(F_{ij}, \varepsilon_q^p)} (G^c M^d - nc_{\sigma - f} nc_{\varepsilon - f} \eta) \tag{2}$$

where $\bar{d}$ is dilatancy, $nc_{\sigma-f}$ is the non-coaxiality between stress and fabric, $nc_{\varepsilon-f}$ is the non-coaxiality between strain and fabric, $F(F_{ij}, \varepsilon_q^p)$ is the state of

fabric evolution, and G' is a function expressed by the following equation:

$$G' = \frac{(1+(1/2)\alpha\cos 2(\theta_\sigma - \theta_f))\cos 2(\beta_i - \beta_o)X + \varepsilon_q^p}{C + \varepsilon_q^p} \quad (3)$$

where $(\beta_i - \beta_0)$ is the bedding angle with respect to the major principal stress. Equation (2) shows that the non-coaxiality between the major principal direction of the stress (θ_σ) and the major principal direction of the strain (θ_ε) which are related via the fabric θ_f. In other words, fabric acts like a "bridge" between these two separate parts. The F function in the denominator of equation 2 is a function of fabric which can be shown by the magnitude of anisotropy α and the major direction of fabric θ_f, the following equation is suggested:

$$F(F_{ij}, \varepsilon_q^p) = 2^{(\varepsilon_q / \varepsilon_{q\max})}(0.5)\left(\frac{2-(0.5\alpha\cos 2(\theta_\sigma - \theta_f))}{4+(0.5\alpha\cos 2(\theta_\sigma - \theta_f))}\right) \quad (4)$$

where $\varepsilon_{q\max}$ is the shear strain corresponds to the maximum shear stress. Since the magnitude of anisotropy α and the non-coaxiality approach constant values, equation 2 tends to a constant value in the critical state. Evolution of the anisotropic parameters such as α and θ_f have an important effect on the dilatancy regime. Direct calculation of the fabric parameters is presented in the following section.

3 FABRIC EVOLUTION

The parameters α and θ_f show the status of the fabric and its evolution. These parameters have a great influence on the behavior of the dilatancy equation. Taha & Shaverdi (2014) proposed an equation which can predict the magnitude of α and θ_f in the presence of the non-coaxiality. This equation is obtained from the micro-level analysis. To calculate the α parameter, the magnitude of the shear to normal stress ratio on the spatial mobilized plane (SMP) must be determined. In the triaxial case, for example, τ/p may be obtained from the following equation (Matsuoka & Geka, 1983):

$$\tau/p = \sqrt{\sigma_1/\sigma_3} - \sqrt{\sigma_3/\sigma_1} \quad (5)$$

The parameters α and θ_f may be obtained from the following equations in the presence of non-coaxiality (Taha & Shaverdi, 2014):

$$\alpha = \frac{(\tau/p)\cos\phi_{\mu mob} - \sin\phi_{\mu mob}}{\sin(2\theta_f + \phi_{\mu mob}) - ((\tau/p)\cos(2\theta_f + \phi_{\mu mob}))} \quad (6)$$

$$\dot{\theta}_f = \dot{\theta}_\sigma + (1/2)\cdot d\eta\cdot(\theta_\sigma - \theta_f) \quad (7)$$

where the dot over θ shows the variation. The most important parameter in the above equation is the inter-particle mobilized friction angle, $\varphi_{\mu mob}$. This parameter is obtained from the following equation:

$$\tan^{-1}\left(\frac{\tau}{p}\right) = \frac{\theta_\sigma - \theta_f}{z} + \lambda\left(\frac{\dot{\varepsilon}_v}{\dot{\varepsilon}_q}\right) + \phi_{\mu mob} \quad (8)$$

where z and λ are material constants. Kuhn (2010) and Shaverdi et al. (2014) showed that the variation of α with the shear strain is similar to the variation of shear to normal stress ratio with shear strain.

4 RESULTS AND DISCUSSION

The non-coaxialities between stress-fabric and strain-fabric are established in equation 2. In this equation fabric acts as a bridge-like role to link the stress tensor to the strain tensor. The proposed equation has the essential parameters to include the initial shear stress effects. When the sample subjected to initial static shear stress, it undergoes of the non-coaxiality between stress and deposition angle (or fabric), it can be included through θ_σ and θ_f. In the cyclic case the non-coaxiality can be happen between strain and fabric, it can also be included through θ_ε and θ_f. The changes between compression and extension can be modeled through equations 3 and 4.

Following the above discussion, it may be noted that the presented flow rule (Equation 2) is inclusive of all previously proposed equations and thus more comprehensive.

5 VERIFICATION WITH EXPERIMENTAL TEST

Because of the paucity of laboratory tests in which initial fabric and their alignment is presented for cyclic loading, here verification is demonstrated for static loading with different bedding angles.

Oda et al. (1978) conducted some triaxial tests on fine Toyoura sand ($D_{50} = 0.18$ mm, $c_u = 1.5$). Maximum and minimum void ratios were 0.99 and 0.63, respectively. They used strong particles to ensure minimal particle crushing. The specimens were sunk into a bucket filled with water and inclined at a tilting angle δ. The Toyoura sand was tapped sufficiently to give a specimen having a void ratio within 0.67 to 0.68. Therefore, all the specimens have a same density. Specimens were sheared in the different tilting angle $\delta = 0$, 30°,60° and 90° in triaxial compression test. The microscopic examination in the vertical sections show that the apparent long axes of the particles well aligned parallel to the bedding angle.

The effect of inherent (or initial) anisotropy and induced anisotropy were included in the dilatancy formulation via $\cos 2(\beta_i - \beta_o)$, α and θ_f, respectively. The parameters α and θ_f are obtained from equations 6 and 7 respectively. The full detail about these constants are presented elsewhere (Shaverdi et al. 2014).

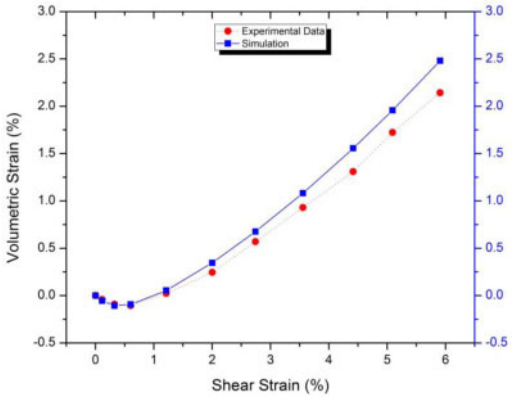

Figure 1. Comparison between experimental data and simulation by using equation 2 for tilting angle $\delta = 0°$ and confining pressure $p_o = 50$ kPa.

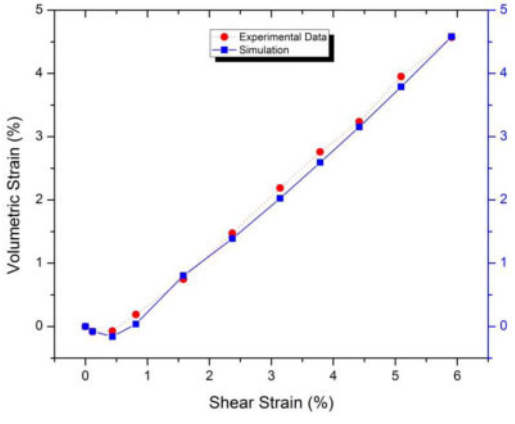

Figure 2. Comparison between experimental data and simulation by using equation 2 for tilting angle $\delta = 90°$ and confining pressure $p_o = 50$ kPa.

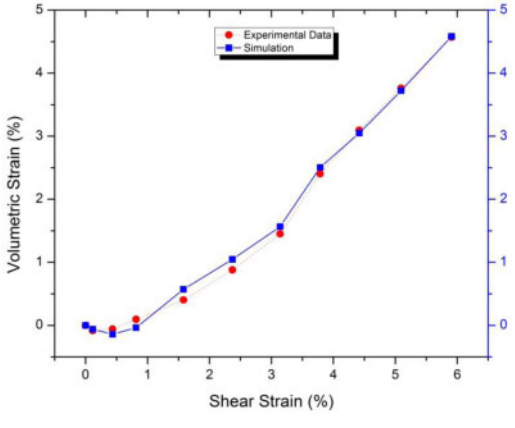

Figure 3. Comparison between experimental data and simulation by using equation 2 for tilting angle $\delta = 30°$ and confining pressure $p_o = 50$ kPa.

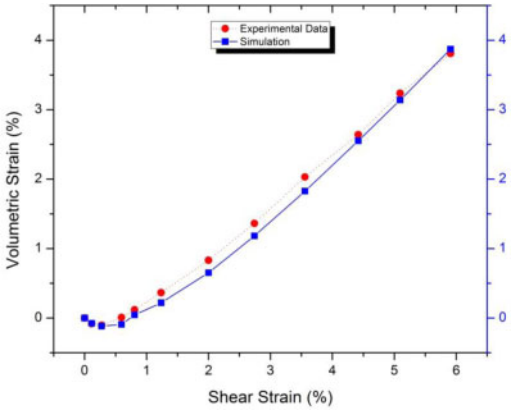

Figure 4. Comparison between experimental data and simulation by using equation 2 for tilting angle $\delta = 60°$ and confining pressure $p_o = 50$ kPa.

Table 1. Constantans that are used for the simulations.

M	1.25
c	0.008
x	0.952
n^d	0

Table 2. Constants used for the evolution of fabric.

Non-coaxiality	z	λ
$\theta_f - \theta_\sigma > 60$	6.29	10
$33 < \theta_f - \theta_\sigma < 60$	4.2	10
$30 < \theta_f - \theta_\sigma < 33$	3.8	10
$23 < \theta_f - \theta_\sigma < 30$	4.2	10
$21 < \theta_f - \theta_\sigma < 23$	5.7	10
$13 < \theta_f - \theta_\sigma < 21$	2.3	10
$11 < \theta_f - \theta_\sigma < 13$	17	10
$\theta_f - \theta_\sigma < 11$	3	10

In figures 1–4 the dilatancy obtained by equation 2 were compared with the experimental tests by Oda et al. (1978). The effects of inherent and induced anisotropy have been included in these simulations. By increasing the tilting angle δ, the magnitude of the parameter α increases with increasing plastic shear deformation, and at the same time, the magnitude of θ_f decreases. The magnitude of $cos\ 2(\beta_i - \beta_o)$ is obtained by back calculation method. The constants used to model the dilatancy are M, n^d, $cos\ 2(\beta_i - \beta_o)$, z, and x that are presented in the tables 1 and 2. The constant M is a classic parameter and easily obtained from experimental data (or from literature for Toyoura sand). Here, the effect of confining pressure was included via the parameter x, hence in this simulation the parameter n^d has been neglected. The effects of inherent and induced anisotropy have been included

in these simulations. By increasing the tilting angle δ, the magnitude of the parameter α increases with increasing plastic shear deformation, and at the same time, the magnitude of θ_f decreases. The difference is due to the variation of the anisotropy parameters (α, θ_f and *cos 2*($\beta_i - \beta_o$)), since at the beginning of shearing the variation of the void ratio in different samples is not a dominant factor. It is obvious that applying these equations with one set of constants can sufficiently model dilatancy in granular material.

6 CONCLUSION

Using micro-level analysis and the principles of thermodynamics a comprehensive flow rule has been proposed in which the effect of initial and induced anisotropy is included. The internal work done by the internal forces and their counterparts strain has been related to the actual applied external loads. The dissipation mechanism in the granular materials was related to the macro-level dissipation mechanism. The applied and dissipation functions defining the contact normals distribution and the internal forces have been adapted from Rothenburg & Bathurst (1989) and Radjai & Azema (2009). The variation of the contact normals or induced anisotropy was related to the variation of the degree of anisotropy α and the direction of the deposition angle of the particles mobilized inside the media, $\cos 2\beta_i$. The parameter $\cos 2(\beta_i - \beta_\circ)$ was applied to show the symbolic limited variation of the initial anisotropy. Verification of the formulation was carried out by simulation of experimental tests conducted by Oda et al. (1978).

REFERENCES

Arangelovski, G., Towhata, I.: Accumulated deformation of sand with initial shear stress and effective stress state lying near failure condition. *Soils & Foundations*, **44**(6):1–16 (2004).

Dafalias, Y.F., Manzari, M.T.: Simple plasticity sand model accounting for fabric change effects. *Journal of Engineering Mechanics*, **130**(6): p. 622–634. (2004).

Finn, W. D. L.: Post-liquefaction flow deformations. In *Soil dynamics and liquefaction 2000 (eds R. Y. S. Pak & J. Yamamura)*, pp. 108–122. Geotechnical Special Publication, No. 107, ASCE (2000).

Gutierrez, M., Ishihara, K., Towhata, I.: Flow theory for sand during rotation of principal stress direction, *Soils and Foundations* **31**(4): 121–132 (1991).

Kuhn, M. R.: Micro-mechanics of fabric and failure in granular materials, *Mechanics of Materials* **42**(9): 827–840 (2010).

Li, X.S., Dafalias, Y.F.: A constitutive framework for anisotropic sand including non-proportional loading, *Geotechnique* **54**(1): 41–55.

Matsuoka, H. and Geka, H.: A stress-strain model for granular materials considering mechanism of fabric change, *Soils and Foundations* **23**(2): 83–97 (1983).

Oda, M.: Initial fabrics and their relations to mechanical properties of granular materials, *Soils and Foundations* **12**(1): 17–36 (1972a).

Oda, M., Koishikawa, I., Higuchi, T.: Experimental study of anisotropic shear strength of sand by plane strain test, *Soils and Foundations* **18**(1): 25–38 (1978).

Radjai, F. and Azema, É.: Shear strength of granular materials, *European Journal of Environmental and Civil Engineering* **13**(2): 203–218 (2009).

Rothenburg, L. and Bathurst, R.: Analytical study of induced anisotropy in idealized granular materials, *Geotechnique* **39**(4): 601–614 (1989).

Shaverdi, H., Taha, M.R., Kalantary, F.: A Flow Rule Incorporating the Fabric and Non-coaxiality in Granular Materials, *Granular Matter*, Under revised.

Taha, M.R., Shaverdi, H.: Evolution of fabric under the rotation of the principal stress axes in the simple shear test, *Mechanics of Materials* **69**(1): 173–184 (2014).

Vaid, Y.P., Chern, J.C.: Effect of static shear on resistance to liquefaction. *Soils & Foundations*, **23**(1): 47–60 (1983).

Vaid, Y.P. Sivathayalan, S.: Static and cyclic liquefaction potential of fraser delta sand in simple shear and triaxial tests, *Canadian Geotechnic Journal* **33**:281–289 (1996).

Vaid, Y.P., Stedman, J.D., Sivathayalan, S.: Confining stress and static shear effects in cyclic liquefaction, *Canadian Geotechnic Journal* **38**:580–591 (2001).

Yoshimine, M., Ishihara, K., Vargas, K., 1998. Effects of principal stress direction and intermediate principal stress on undrained shear behavior of sand. *Soils and Foundations* **38**(3): 179–188.